



Preparation and investigation of a novel iodine-based visible polyvinyl alcohol embolization material



Yupeng Yang^a, Rui Yang^a, Beilei Zhang^a, Ye Tian^c, Yanqi Lu^c, Xiao An^{b,**}, Xiangyang Shi^{a,*}

^a State Key Laboratory for Modification of Chemical Fibers and Polymer Materials, Shanghai Engineering Research Center of Nano-Biomaterials and Regenerative Medicine, College of Chemistry, Chemical Engineering and Biotechnology, Donghua University, Shanghai, 201620, China

^b Department of Neoplasms and Interventional Radiology, Shanghai General Hospital, Shanghai Jiao Tong University School of Medicine, Shanghai, 200080, China

^c Department of Pharmacy, Zhengzhou Railway Vocational & Technical College, Zhengzhou, 451460, China

ARTICLE INFO

Keywords:

Electrospinning
PVA/Gelatin/I embolic material
Fiber blocks
Visualization
Embolization

ABSTRACT

Polyvinyl alcohol (PVA) embolization particles, currently used in clinical practice, have good expansibility and are capable of permanent embolization. However, the lack of adhesion of embolization particles contributes to facilitated recanalization after embolization, while the lack of visualization facilitates misembolization. At present, embolization materials with good expansion, adhesion, and visualization potential are urgently required in clinical practice. Here, we report the development of PVA/gelatin/iodohexol (I) fiber blocks as a novel embolization material for liver embolization in rats. In our work, electrospun PVA/gelatin/I nanofibrous mats were first prepared, homogenized, centrifuged in a gradient manner, and freeze-dried to obtain fiber blocks (fiber diameter = 296.2 ± 74.23 nm, length 99.6 ± 17.0 μm \times width 46.9 ± 13.3 μm). The fiber blocks exhibited excellent cytocompatibility and hemocompatibility. Fiber blocks with a PVA/gelatin/I mass ratio of 8:2:10 were selected due to their excellent expansibility and adhesive properties. The PVA/gelatin/I fiber blocks display excellent liver embolic effects and computed tomography (CT) imaging potential due to a combination of the following characteristics: expansibility of PVA and gelatin, adhesive property of gelatin, and CT imaging potential of I. The developed fiber block material is an embolic material that may potentially be used in interventional medicine.

1. Introduction

Interventional radiology is a field of medicine which has seen major breakthroughs and advances since the second half of the 20th century.^{1–5} In this century, the continuous emergence of more advanced equipment, including finer guidewire catheters and stronger stents, has significantly facilitated the development of clinical intervention. Arterial embolization, one of the most important components of interventional therapy, requires the injection of embolic material into the target tissue through a catheter inserted into the target blood vessel to achieve precise embolization.⁶ The ideal embolic material should be non-toxic, non-antigenic, capable of quickly occluding blood vessels of different calibers, easily injected, non-sticky, and easily visualized or tracked. However, the application of arterial embolization is hindered due to the lack of desired embolization materials.^{7,8}

Gelatin sponges, commonly used in clinical practice, can be transformed into particles of different sizes and embolized in different

branches for specific conditions, which is convenient and facilitates their use in clinical practice. However, it is difficult to achieve the effect of terminal embolization, and blood vessels are easily recanalized after embolization due to the lack of solidity in gelatin sponges.⁹ Theoretically, although anhydrous ethanol can achieve terminal and permanent embolization, the dose and rate of injection are difficult to control, and an excessive dose can lead to extensive necrosis of normal tissues and other serious complications.^{10,11} The Guglielmi detachable coil, a permanent embolization material, can only be applied for embolization of large branches of a blood vessel and may induce thrombosis of non-embolized branches due to its metallic texture. Due to the tumorigenic nature of lipiodol, the combined use of lipiodol and chemotherapeutic drugs can significantly increase the residence time of the drug in the lesion, which facilitates its use in the interventional treatment of malignant solid tumors. However, lipiodol is mucous and easily excluded after embolizing tumor blood vessels, and the residence time in tumor tissue is limited. Therefore, target blood vessels are not completely

* Corresponding author.

** Corresponding author.

E-mail addresses: drxiaoan@126.com (X. An), xshi@dhu.edu.cn (X. Shi).

<https://doi.org/10.1016/j.jimed.2022.03.009>

Received 9 January 2022; Received in revised form 10 March 2022; Accepted 10 March 2022

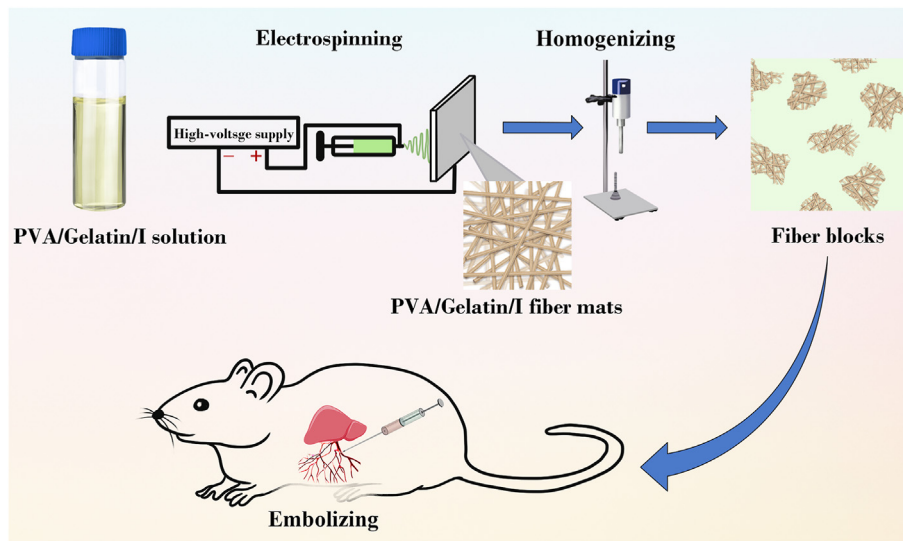


Fig. 1. Fabrication and embolic application of the PVA/gelatin/iohexol fiber blocks.

embolized with the use of this material. In addition, an excessive dose of lipiodol can cause discomfort in some patients.

Currently, polyvinyl alcohol (PVA) with good biocompatibility has been considered a promising terminal permanent embolization agent^{12–15} and is commercially available (e.g., PVA Particle Embolic Agent, Hangzhou Alicon Pharm SCI&TEC Co., Ltd.) for use in interventional clinical practice. However, the limitations of PVA are also apparent. For example, PVA particles without imaging ability must be mixed with an imaging contrast agent before embolization to prevent serious complications caused by accidental embolization. Additionally, the embolization mechanism of PVA is based on mechanical dilation after water absorption, and the material lacks adhesion. In addition, the size of the lumen of the target blood vessels *in vivo* is altered based on changes in pressure, thus causing vascular recanalization after PVA embolization, which severely limits its long-term effectiveness.

Based on the computed tomography (CT) imaging ability of iohexol (I) and the good adhesion property of gelatin, we propose the design of a multifunctional PVA-based embolic material with visualization and adhesion properties by integrating PVA with I and gelatin.¹⁶ PVA with appropriate molecular weight was selected and dissolved in water to obtain a uniform solution, and then mixed with a gelatin/I solution at a given concentration, followed by electrospinning to create composite fibrous mats with different PVA/gelatin/I ratios.^{17–20} By comparing the structure, adhesion, and expansion properties of different fiber mats, a fiber mat with a PVA/gelatin/I ratio of 8:2:10 was selected for the preparation of fiber blocks. The fibrous mats were homogenized and processed by gradient centrifugation to create a multifunctional embolic material with good adhesion and CT imaging potential for embolization of the liver in rats (Fig. 1). The developed PVA/gelatin/I fiber blocks were thoroughly characterized and evaluated in terms of their hemocompatibility, cytocompatibility, CT imaging, and embolization properties. To our knowledge, this is the first example of the development of an embolic material based on fiber blocks.

2. Materials and methods

2.1. Preparation and crosslinking of electrospun fiber mats

PVA (0.8 g) was dissolved in water (5 mL) and stirred at 85 °C for 3 h. The gelatin/I solution was obtained by dissolving gelatin (0.2 g) in I solution (4 mL) under stirring at 45 °C for 0.5 h. After both solutions were cooled to room temperature, the gelatin/I solution was blended with the PVA solution to form a homogeneous suspension. Electrospinning was

performed to generate a PVA/gelatin/I fibrous mat by using a 19-gauge needle under the optimized conditions of applied voltage of 21 kV, flow rate of 0.5 mL/h, collecting distance of 14 cm, ambient temperature of 25 °C, and humidity of 55%. Under the same conditions, fiber mats with different PVA/gelatin/I ratios (pure PVA, PVA/gelatin/I = 9:1:10 or 7:3:10) were obtained and further crosslinked by glutaraldehyde (GA) vapor. The process was as follows: 10 mL of GA aqueous solution (36%) and 10 mL of concentrated hydrochloric acid were placed at the bottom of a vacuum dryer, while the fibrous mats were placed on the upper side of the dryer, which was evacuated for 2 min to generate vapors of GA and hydrochloric acid to crosslink the fibrous mats for 2 h at room temperature.

2.2. Preparation and screening of fiber blocks

The crosslinked fiber mats were homogenized (24,000 rpm, 40 min) and then separated by gradient centrifugation (5000, 3000, and 1500 rpm, 80 s each time). After each centrifugation step, the supernatant was collected, and a drop of the suspension was placed on a glass slide to observe the size and morphology of the fiber blocks using a Leica DM IL LED inverted phase contrast microscope (Wetzlar, Germany). Based on gradient centrifugation, the optimized centrifuge condition (1500 rpm, 80 s) was adopted to obtain the desired dimensions of the fiber blocks. To determine the amount of I in the fiber blocks, the crosslinked fiber blocks were digested with *aqua regia* for 4 h, diluted 25 times with water, and sonicated for 20 min, followed by quantification using Leeman Prodigy inductively coupled plasma-optical emission spectroscopy (ICP-OES, Hudson, NH).

2.3. Cytotoxicity assay

The *in vitro* cytotoxicity of the PVA/gelatin/I fiber blocks was evaluated using a standard cell counting kit-8 (CCK-8) cell viability assay. In brief, HUVECs (human umbilical vein endothelial cells) were seeded into a 96-well plate at a density of 1×10^4 cells per well in 0.1 mL medium and cultured overnight at 37 °C and 5% CO₂. The next day, the medium in each well was replaced with fresh medium containing PVA/gelatin/I fiber blocks at different concentrations (0, 1, 2, 4, and 8 mg/mL). After 24 h, the cells were washed thrice with phosphate-buffered saline (PBS) and treated with 100 μ L of medium containing 10% CCK-8 for an additional 3 h. The absorbance of each well was read using a Thermo Scientific Multiskan MK3 ELISA reader (Waltham, MA, USA) at 450 nm.

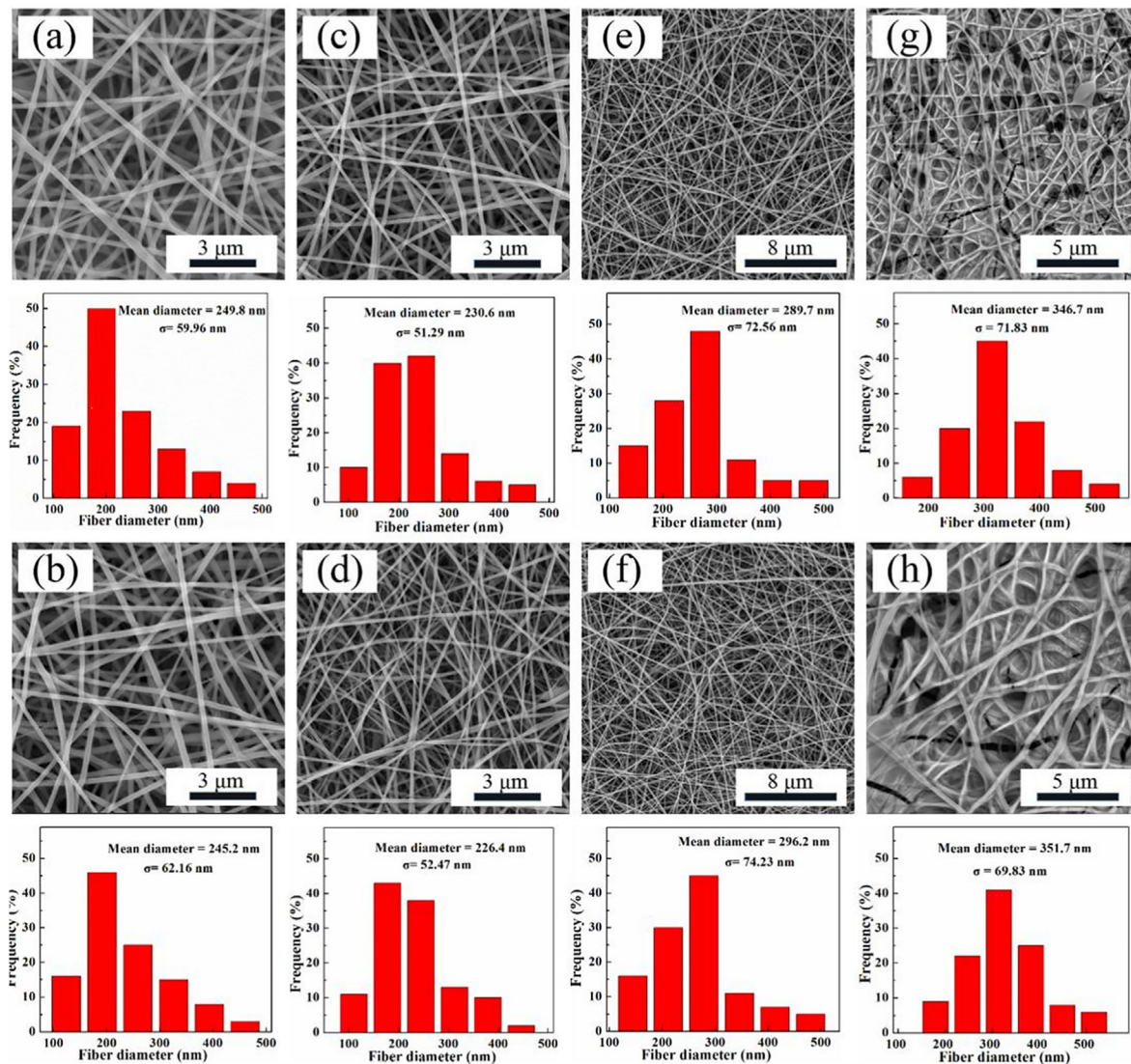


Fig. 2. SEM images and fiber diameter distributions of four fiber mats with different PVA/gelatin/I ratios (pure PVA (a, b), PVA/gelatin/I = 9:1:10 (c, d), 8:2:10 (e, f), and 7:3:10 (g, h), respectively) before (a–g) and after (b–h) GA-vapor crosslinking.

2.4. Animal embolization tests

All animal experiments were performed after approval by the Institutional Animal Care and Use Committee of Shanghai General Hospital (IACUC 2019-A018-01), Shanghai Jiao Tong University School of Medicine, and in accordance with the policy of the National Ministry of Health. Healthy adult Sprague-Dawley rats (average weight of 280 g per rat) were purchased from Beijing Vital River Laboratory Animal Technology Co., Ltd. (Beijing, China). The rats were divided into two groups ($n = 6$ for each group) and were treated by embolization of the liver with the prepared PVA/gelatin/I fiber blocks (Group A) and commercial medical PVA embolization particles (150–350 μm , Hangzhou Alicon Pharm SCI&TEC Co., Ltd., Hangzhou, China) of the same size as that of the fiber blocks (Group B).

Before surgery, the materials used in groups A and B were disinfected by overnight exposure to an ultraviolet lamp. The specific steps were as follows. First, Groups A and B were further divided into three subgroups ($n = 2$ for each group) and marked based on the injection dose (10, 20, and 40 mg, respectively, Table S3). After each rat was anesthetized with 10% pentobarbital sodium, the abdomen was incised, and the suspension containing embolic material was injected into the superior mesenteric vein of the rat with a syringe for embolization of the liver. The suspension

was prepared at a concentration of 15 mg/mL to prevent clogging of the needle. The amount of material in the experimental group was based on that of gelatin and PVA used in the fiber blocks. After injection of embolic material into the superior mesenteric vein, the blood vessels and abdomen were quickly sutured. The postoperative mice were fed and monitored regularly. Liver specimens were removed using the spinal cord dissection method after the embolization test and used for hematoxylin and eosin (H&E) staining.

3. Results and discussion

3.1. Preparation and characterization of PVA/gelatin/I fiber materials

In this study, we prepared four different fibrous mats with different PVA/gelatin/I mass ratios using electrospinning technology (PVA/gelatin/I = 9:1:10, 8:2:10, or 7:3:10 and pure PVA) and crosslinked them using GA vapor based on our previous report.²¹ The fiber materials before and after crosslinking were characterized using scanning electron microscopy (SEM) and Fourier transform infrared (FTIR) spectroscopy.

As shown in Fig. 2, the mean diameters of the fiber mats with different PVA/gelatin/I mass ratios (pure PVA, PVA/gelatin/I = 9:1:10, 8:2:10, 7:3:10) before crosslinking were 249.8 ± 59.96 nm, $230.6 \pm$

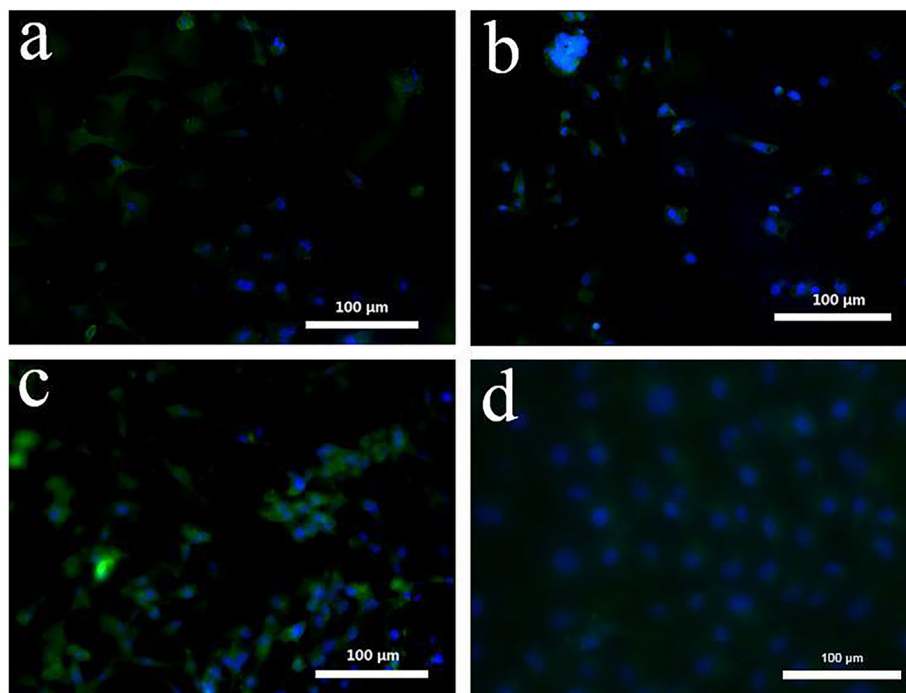


Fig. 3. Fluorescence microscopic images of HUVECs treated with four fiber mats with different PVA/gelatin/I mass ratios ($400\times$, pure PVA (a), PVA/gelatin/I = 9:1:10 (b), 8:2:10 (c), and 7:3:10 (d)).

51.29 nm, 289.7 ± 72.56 nm, and 346.7 ± 71.83 nm, respectively. The morphologies and structures of the fiber mats did not exhibit appreciable changes after crosslinking. The fiber diameter tended to decrease first and then increase with an increase in the gelatin content, likely due to an increase in gelatin content, which led to a decrease in the viscosity of the electrospinning liquid, making it easier for the liquid to be fully stretched under a high-voltage electric field. In addition, the conductivity of the system gradually became unstable during the electrospinning process. After the conductivity of the electrospinning solution increased to a certain level, many droplets left the apex of the cone and aggregated on the needle to intermittently form fibers, causing an increase in fiber diameter. When the gelatin content exceeded 20% of the total amount of PVA and gelatin, the morphology of the fibers deteriorated (Fig. 2g) due to the poor mutual solubility of PVA and gelatin. Moreover, FTIR spectra were acquired to investigate the structure of the fiber mat (PVA/gelatin/I = 8: 2: 10) before and after crosslinking (Figure S1). Compared with the fiber mat before crosslinking, the -OH characteristic absorption peak for the crosslinked PVA/gelatin/I fiber mat at 1647 cm^{-1} disappeared. There were characteristic peaks of -CHO and -(C=O)- at 1698 cm^{-1} , suggesting that PVA and GA may react under acidic catalysis to form acetal or hemiacetal bonds. Furthermore, after crosslinking, the fibrous mats displayed excellent water stability, in contrast to the pristine non-

crosslinked fibrous mats that are quickly soluble in water, indicating successful crosslinking of PVA and GA to create water-stable fibrous mats.

3.2. Screening of fiber materials

Good swelling and adhesion properties are considered the main evaluation indicators of embolic materials, which enable the material to rapidly and firmly embolize the target vessel and seal vascular bleeding. PVA, as an embolic material with good expansion properties, is prone to recanalization due to the absence of adhesion after embolization. However, gelatin, with its swellability and adhesive properties, may play a role in increased adhesion. Therefore, we incorporated an appropriate amount of gelatin into the fiber materials for increased swellability, while simultaneously improving their adhesive property.

First, the water absorption ability of the fibrous mat was tested to investigate the swelling properties of the four types of mats. We measured the masses of the fibrous mats before and after soaking them in water for 30 min to determine their water absorption rates (Table S1). The water absorption rate of the pure PVA fibers was only 76.7%. The water absorption rate of the fiber materials increased with increasing gelatin content, indicating the significant expansion performance of the

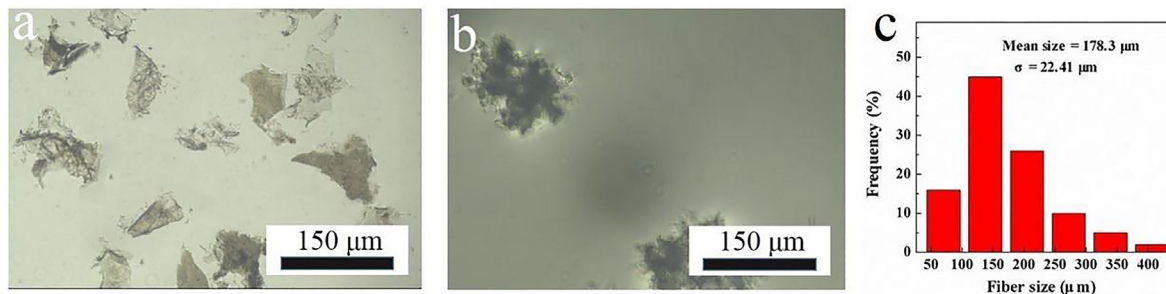


Fig. 4. Microscopic images of the fiber blocks (PVA/gelatin/I = 8:2:10) in the supernatant under the condition of 1500 rpm centrifugation (80 s) (a), and medical PVA embolization particles (b) with a particle size of 150–350 μm (length $168.1 \pm 17.0\ \mu\text{m}$ \times width $119.6 \pm 16.0\ \mu\text{m}$). (c) Size distribution histogram of the fiber blocks.

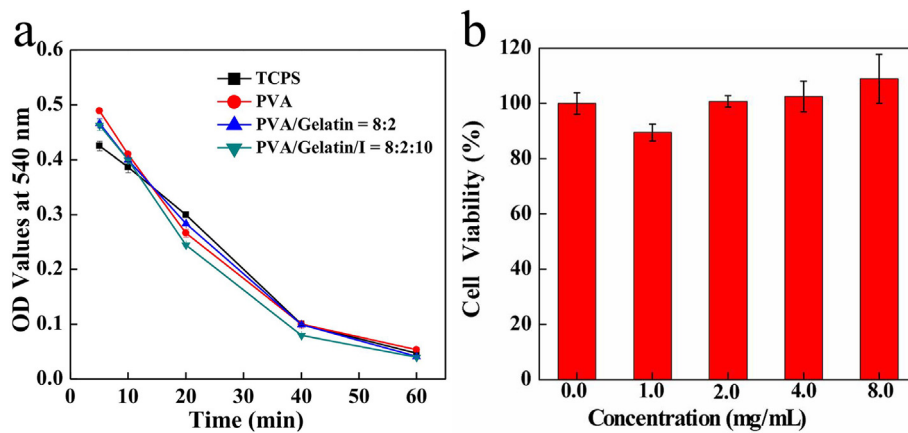


Fig. 5. OD values at 540 nm for anticoagulant assay of TCPS, PVA, PVA/gelatin = 8:2, and PVA/gelatin/I = 8:2:10 fiber blocks at different time intervals (a). Viability of HUVECs after treatment with fiber blocks (PVA/gelatin/I = 8:2:10) at different concentrations for 24 h (n = 5) (b).

PVA/gelatin/I fiber material.

Furthermore, the adhesive properties of the four fibrous mats were tested by checking cell adhesion to the mats. As depicted in Fig. 3 and Figure S2, with increased gelatin content in the fiber mats, more cells were attached to the fiber mats, proving that high gelatin content leads to improved cell adhesion of the fiber materials. Combined with the results of the swelling tests, we showed that the fiber mat composed of PVA/gelatin/I at a mass ratio of 7:3:10 was the best in terms of swellability and adhesive property. Excessive gelatin content leads to failure to form fibers with a uniform fibrous morphology (Fig. 2g) during electrospinning. In addition, the high gelatin content causes excessive viscosity, making it difficult to shear the fiber mat during the preparation of the fiber blocks, and subsequently causes over-adhesion of tubes, making the embolization operation difficult. Therefore, the fiber material with a PVA/gelatin/I mass ratio of 8:2:10 was selected for subsequent experiments.

3.3. Preparation and screening of fiber blocks

The selected fiber mat (PVA/gelatin/I mass ratio = 8:2:10) was subjected to high-speed shearing, gradient centrifugation, and freeze-drying to obtain fiber blocks with dimensions in the range of 50–350 μm (Fig. 4a), which is similar to the size of medical PVA embolization particles (Fig. 4b). To further investigate the composition of the fiber blocks, the iodine content in the freeze-dried fiber blocks was determined to be 25% by inductively coupled plasma-optical emission spectroscopy (ICP-OES).

3.4. Blood compatibility and cell viability tests

Hemocompatibility must be considered for any material implanted in the human body. Hemolysis assays were performed to check the hemocompatibility of the PVA, PVA/gelatin (mass ratio = 8:2), and PVA/gelatin/I (mass ratio = 8:2:10) fiber blocks to prove their usability. As shown in Table S2, the hemolysis rates of all fiber blocks with three concentration gradients (2, 4, and 6 mg/mL) were less than 5%, suggesting good hemocompatibility of the developed fiber blocks.

In addition, severe coagulation causes local tissue necrosis or even death. Dynamic coagulation assay was employed to evaluate the anticoagulant property of the fibrous mats. As depicted in Fig. 5a, the optical density (OD) values of the PVA, PVA/gelatin, and PVA/gelatin/I fiber mats were slightly lower than those of the control group (tissue culture plates, TCPS) within 15–40 min of the same time point, suggesting that the fiber blocks may accelerate blood coagulation for a period of time, but within an acceptable range. However, coagulation of the fiber block and control groups remained consistent over 40–60 min, demonstrating that the fiber blocks were endowed with good anticoagulant properties.

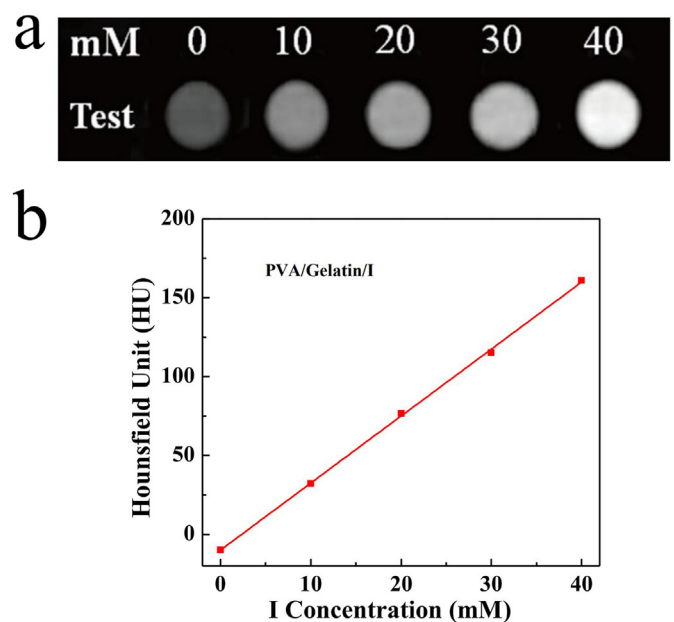


Fig. 6. CT images of PVA/gelatin/I fiber blocks in saline at different I concentrations (a), and corresponding linear fitting of HU value versus I concentration (b).

Collectively, we can safely conclude that the prepared fiber blocks exhibit excellent hemocompatibility.

The viability of HUVECs treated with different concentrations of fiber blocks (PVA/gelatin/I mass ratio = 8:2:10) at different concentrations for 24 h was tested to determine the cytocompatibility of the fiber blocks (n = 5). The cell viability hardly decreased in the fiber block concentration range of 0–8 mg/mL (Fig. 5b), suggesting good cytocompatibility. Interestingly, when the concentration was higher than 4 mg/mL, cell viability exceeded 100%, implying that the fiber blocks can promote HUVEC growth due to the presence of gelatin and a unique porous structure.

3.5. In vitro CT imaging

Afterward, to test the potential of using the PVA/gelatin/I fiber blocks for CT imaging, we performed a CT phantom investigation of the fiber blocks with different I concentrations. As shown in Fig. 6a and b, the fiber blocks exhibited an I concentration-dependent increase in CT imaging brightness and X-ray attenuation intensity. This suggests that with the

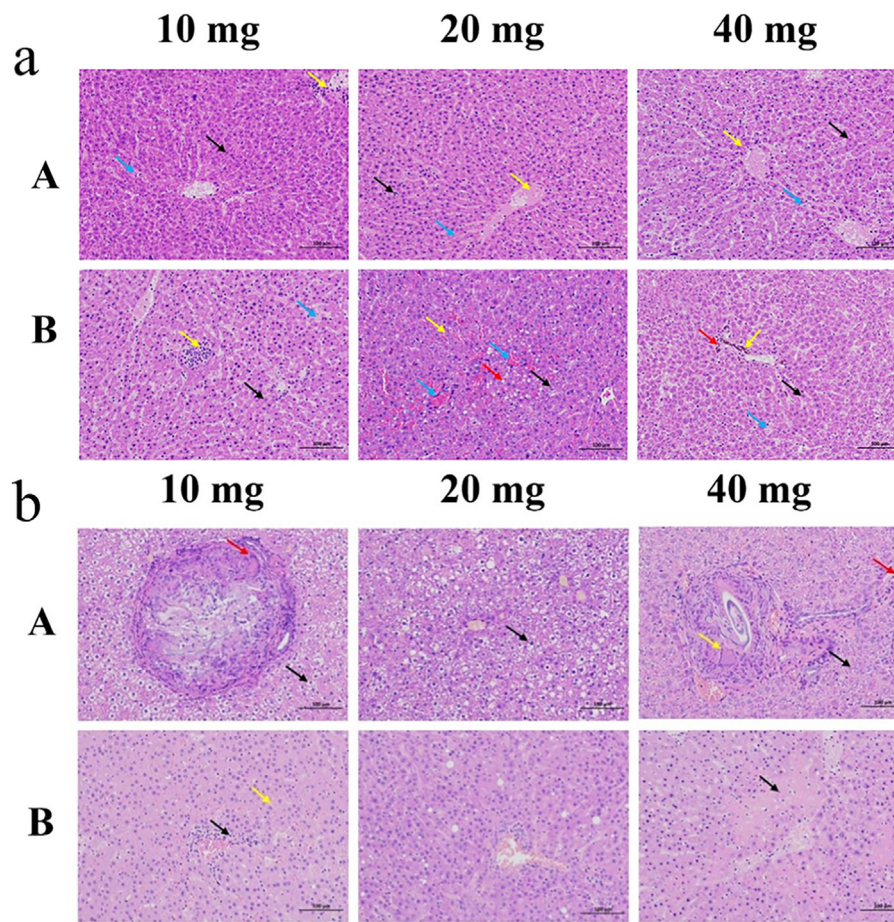


Fig. 7. H&E staining of rat liver after embolization with different injection amounts of PVA/gelatin/I fiber blocks (A) and medical PVA embolization particles (B) (focusing on the analysis of histological structure (a) and cell structure (b)).

incorporation of I, the PVA/gelatin/I fiber blocks may hold great promise for use in CT imaging applications.

3.6. Animal embolism test

An embolism test was performed on the liver of healthy rats to check the embolization properties of the PVA/Gelatin/I fiber blocks. On the first day after the embolism operation, we collected the livers of three rats in the control group (B2, B4, and B5) that died. On postoperative day 14, B1 died, and necropsy revealed severe intra-abdominal decomposition and a large amount of feces in the abdominal cavity, which can be attributed to postoperative ischemic intestinal necrosis or intestinal fistula. B6 died on postoperative day 17, while the remaining animals had normal development. The remaining seven liver specimens (A1–A6 and B3) were dissected using the spinal cord dissection method on postoperative day 18 and preserved in formalin solution. Later, 10 liver tissue samples (A1–A6 and B2–B5) were obtained and H&E stained (Fig. 7).

As depicted in Fig. 7a, histological analysis of the experimental group injected with 10 mg of fiber blocks revealed a large amount of hepatocyte necrosis. Nuclear pyknosis or fragmentation (black arrow), lymphocyte infiltration (yellow arrow) in the liver section, and hepatic sinusoids filled with eosinophilic fluid (blue arrow) were observed. In the experimental group injected with 20 mg of fiber blocks, we found that the liver cord arrangement was not clear, and the number of white blood cells in the local liver sinusoids increased slightly (black arrow). Necrosis with nuclear fragmentation or dissolution of venous vascular epithelial cells (yellow arrow) can be seen locally in this section. Similarly, the hepatic sinusoids are filled with eosinophilic fluid (blue arrows). Moreover, in the experimental group injected with 40 mg of fiber blocks, a large

amount of hepatocyte necrosis with nuclear pyknosis or fragmentation (black arrow) was also widely visible in the tissue. Simultaneously, lymphocyte punctate infiltration can be seen around the blood vessels (yellow arrow), and the hepatic sinusoids are filled with eosinophilic fluid (blue arrow).

For comparison, the histological structure of the control group injected with 10 mg of medical PVA embolization particles was also analyzed. The results are as follows: hepatocyte necrosis (black arrow), lymphocyte focal infiltration (yellow arrow), a specific amount of necrotic cell debris in the local vascular lumen of the portal vein in the portal area, and eosinophilic fluid filled with hepatic sinusoids (blue arrow) were observed. In the control group injected with 20 mg of medical PVA embolization particles, we found a large amount of hepatocyte edema with cytoplasmic looseness and light staining (black arrow) in the tissue, more hepatocyte necrosis with pyknosis, dark staining, or fragmentation (yellow arrow) in local tissues, swollen hepatocytes with vacuolated cytoplasm (red arrow), and congestion and expansion of the liver sinusoids and portal vein in the portal area (blue arrow). In the group injected with 40 mg of medical PVA embolization particles, there was also significant hepatocyte necrosis with nuclear pyknosis or fragmentation (black arrow), brown-yellow particles in the tissue (yellow arrow), lymphocyte infiltration around the portal vein in the portal area (red arrow), and eosinophilic fluid filled with the liver sinusoids (blue arrow).

Based on the analysis of the cell structure of the experimental group injected with 10 mg of fiber blocks (Fig. 7b), we found many swollen hepatocytes with centered nuclei and vacuolated cytoplasm (black arrow), a granuloma wrapped by connective tissue, and multinucleated giant cells (red arrow). When the injection dose was increased (20 and

40 mg), many swollen hepatocytes with vacuolated cytoplasm (black arrow) were observed. Furthermore, at an injection dose of 40 mg, the granulomas were encapsulated with a thin layer of connective tissue in the bile duct area (yellow arrow), and punctate infiltration of lymphocytes (red arrow) was noted. In the control group injected with 10 mg of medical PVA embolization particles, a neatly arranged hepatic cord (black arrow) and punctate infiltration of lymphocytes around the bile duct in the portal area (yellow arrow) were observed. We found increased hepatocyte steatosis (20 mg control group) and hepatocyte necrosis with nuclear fragmentation or lysis (black arrow, 40 mg control group) with increased injection dose. Compared to medical PVA embolization particles, the developed PVA/gelatin/I fiber blocks exhibit similar embolic effects in rats, which is attributed to the low gelatin content in the fiber block or the short embolization time, resulting in a lack of benefit associated with gelatin adhesion.

4. Conclusion

In conclusion, we developed a novel PVA/gelatin/I fiber block embolization material that combines expansion, adhesion, and CT imaging potential for embolization of the liver in rats by homogeneous shearing, gradient centrifugation, and freeze-drying. Comparing the morphology, expansion, and adhesion properties of embolic materials with different PVA/gelatin/I mass ratios, we show that the embolic material with a mass ratio of 8:2:10 is optimal. Moreover, based on the natural composition of gelatin and the unique porous structure of the fiber block, the PVA/gelatin/I fiber blocks possess good cytocompatibility. Although the PVA/gelatin/I fiber blocks showed similar embolization effects in rats compared to medical PVA embolization particles, they have unique CT imaging potential for visualization of the embolism. Overall, the designed fiber block, a powerful imaging-guided embolization platform, may be further modified with other imaging agents and therapeutic elements to achieve visualized embolization therapy.

Institutional review board statement

The study was conducted according to the guidelines of the Declaration of Helsinki, and approved by the Institutional Animal Care and Use Committee of Shanghai General Hospital (IACUC 2019-A018-01), Shanghai Jiao Tong University School of Medicine.

Informed consent statement

Not applicable.

Data availability statement

Not applicable.

Declaration of competing interest

The authors declare no conflict of interest.

Acknowledgments

The authors acknowledge the support of the State Key Laboratory for

Modification of Chemical Fibers and Polymer Materials, Donghua University, the Science and Technology Commission of Shanghai Municipality (19XD1400100 and 20520710300), the 2019th Shanghai Medical Guide Science and Technology Supporting Project (19411971000), and the Science and Technology Research Project from the Science and Technology Department of Henan Province in 2020 (202102310539).

Appendix A. Supplementary data

Supplementary data to this article can be found online at <https://doi.org/10.1016/j.jimed.2022.03.009>.

References

1. Durack JC. The value proposition of structured reporting in interventional radiology. *AJR Am J Roentgenol.* 2014;203:734–738.
2. Higgins MCSS, Beeram IR. The imperative for diversity and inclusion in interventional radiology. *AJR Am J Roentgenol.* 2021;217:761–764.
3. Sheth RA, Sabir S, Krishnamurthy S, et al. Endovascular embolization by transcatheter delivery of particles: past, present, and future. *J Funct Biomater.* 2017;8:12.
4. Small W, Buckley PR, Wilson TS, et al. Shape memory polymer stent with expandable foam: a new concept for endovascular embolization of fusiform aneurysms. *IEEE Trans Biomed Eng.* 2007;54:1157–1160.
5. Park JM, Lee SY, Lee GH, et al. Design and characterisation of doxorubicin-releasing chitosan microspheres for anti-cancer chemoembolisation. *J Microencapsul.* 2012;29:695–705.
6. Rosenbluth PR, Grossman R, Arias B. Accurate placement of artificial emboli. A problem in the treatment of cerebral angiomas by the embolization method. *JAMA.* 1960;174:308–309.
7. Jia JB, Green CS, Cohen AJ, et al. CT and radiographic appearance of extracranial Onyx(®) embolization. *Clin Radiol.* 2015;70:326–332.
8. Poursaid A, Jensen MM, Huo E, et al. Polymeric materials for embolic and chemoembolic applications. *J Controlled Release.* 2016;240:414–433.
9. Coldwell DM, Stokes KR, Yakes WF. Embolotherapy: agents, clinical applications, and techniques. *Radiographics.* 1994;14:623–643.
10. Burrows PE, Mason KP. Percutaneous treatment of low flow vascular malformations. *J Vasc Intervent Radiol.* 2004;15:431–445.
11. Do YS, Yakes WF, Shin SW, et al. Ethanol embolization of arteriovenous malformations: interim results. *Radiology.* 2005;235:674–682.
12. Chung JW. Transcatheter arterial chemoembolization of hepatocellular carcinoma. *Hepato-Gastroenterology.* 1998;45:1236–1241.
13. Liu YS, Lin XZ, Tsai HM, et al. Development of biodegradable radiopaque microsphere for arterial embolization-a pig study. *World J Radiol.* 2015;7:212–219.
14. Liu QS, Mei QL, Li YH. Polyvinyl alcohol terminal chemoembolization for hepatocellular carcinoma with hepatic arteriovenous shunts: safety, efficacy, and prognostic factors. *Eur J Radiol.* 2017;89:277–283.
15. Niu C, Chen M, Shen G, et al. Transcatheter arterial sclerosis and embolization with bolemicin lipiodol emulsion and polyvinyl alcohol in the treatment of infantile hepatic hemangioma. *Chin J Radiol.* 2017;51:206–209.
16. Fan L, Duan M, Xie Z, et al. Injectable and radiopaque liquid metal/calcium alginate hydrogels for endovascular embolization and tumor embolotherapy. *Small.* 2020;16:e1903421.
17. Wang S, Zhu J, Shen M, et al. Poly(amidoamine) dendrimer-enabled simultaneous stabilization and functionalization of electrospun poly(γ -glutamic acid) nanofibers. *ACS Appl Mater Interfaces.* 2014;6:2153–2161.
18. Zhang CL, Yu SH. Nanoparticles meet electrospinning: recent advances and future prospects. *Chem Soc Rev.* 2014;43:4423–4448.
19. Nascimento ML, Araújo ES, Cordeiro ER, et al. A literature investigation about electrospinning and nanofibers: historical trends, current status and future challenges. *Recent Pat Nanotechnol.* 2015;9:76–85.
20. Saallah S, Naim MN, Lenggono IW, et al. Immobilisation of cyclodextrin glucanotransferase into polyvinyl alcohol (PVA) nanofibres via electrospinning. *Biotechnol Rep (Amst).* 2016;10:44–48.
21. Xiao YC, Lin LZ, Shen MW, et al. Design of DNA aptamer-functionalized magnetic short nanofibers for efficient capture and release of circulating tumor cells. *Bioconjugate Chem.* 2020;31:130–138.